Hindawi
Advances in Materials Science and Engineering
Volume 2022, Article ID 3925520, 10 pages
https://doi.org/10.1155/2022/3925520

Research Article

Design and Performance Evaluation of Dry-Mixed Cement Recycled Aggregate Pile

Boming Shang,[1,2] **Feng Jin**,[1,2] **Xuewen Rong**,[1,2] **Shanjun Wang**,[1,2] **Qi Zhang**,[1,2] **Zhen Wang**,[1,2] **and Kang Yao**[1,2]

[1]*Shaanxi Zhengcheng Road and Bridge Engineering Research Institute Co. LTD, Xi'an 710065, China*
[2]*Shaanxi Huashan Road and Bridge Group Co. LTD, Xi'an 710065, China*

Correspondence should be addressed to Boming Shang; bomingshang@163.com

Received 3 May 2022; Accepted 23 June 2022; Published 11 July 2022

Academic Editor: Bowen Guan

In this paper, dry-mixed recycled cement concrete gravel (CCG) piles and dry-mixed cement macadam gravel (CMG) piles were analyzed. CCG and CMG were prepared by using recycled concrete aggregate (RCA) with different substitution rates, recycled macadam aggregate (RMA) from waste bricks and tiles, and fly ash, respectively. Mechanical properties, hydration heat release performance, and frost resistance were used as evaluation factors. The compressive strength, hydration heat, relative dynamic elastic modulus, and mass loss rate were tested. Based on the requirements of subgrade reinforcement on the material strength, hydration heat release, and frost resistance of dry-mixed CRA piles, TOPSIS analysis method was used to conduct a comprehensive evaluation. The results show that the mechanical properties and frost resistance of CCG and CMG gradually deteriorate with the increase of RCA and RMA replacement rates. At the same time, the hydration heat release of CCG and CMG increases with the increase of the replacement rate. The fly ash instead of cement can improve the compressive strength and frost resistance of CCG and CMG and reduce the hydration heat and material cost. When the CCG replacement rate reaches 20%, the CCG composite score of 20% fly ash is higher than that of traditional dry-mixed cement gravel pile and has better comprehensive performance.

1. Introduction

In recent years, with the large-scale construction of high-grade highway, the problems encountered in the project have become more frequent and complex. Soft soil foundation has the characteristics of high compressibility, large settlement, and poor stability of drainage consolidation. Before building high-grade highway on such foundations, if the foundations are not treated or improper treatment, the quality of the highway will be reduced or even destroyed [1]. As a result, a series of problems such as pavement subsidence, muddying, pulping, bridge jumping, and roadbed slippage appear [2]. Dry-mixed cement gravel pile is a new trenchless rapid reinforcement technology for highway subgrade developed based on gravel pile and cement fly-ash gravel (CFG) pile [3]. This technology has the advantages of simple process, low equipment requirements, local materials for raw materials, high overall strength formed with the original topography, and effective suppression of the unstable settlement of roadbed. Along with the rapid development of highway traffic construction, construction engineering, water conservancy, and other infrastructure construction industry, the rapid development of engineering construction in the aggregate supply gap is gradually expanding [4]. However, a series of environmental problems will be caused in the process of large-scale construction. In order to solve the problem of environmental pollution caused by aggregates shortage in engineering construction, waste aggregates recycling has become an effective solution [5].

The research on recycled waste concrete materials has become a hot topic for scholars in related fields. Many scholars have studied the properties of recycled aggregate (RA) and recycled concrete. Bai et al. investigated the characteristics of RA and the mechanical properties of recycled concrete [6]. Some scholars have conducted comparative studies on the mechanical properties of

(a) (b)

Figure 1: Macroscopic view of RA. (a) RCA, (b) RMA.

ordinary concrete and recycled concrete [7]. The research results generally show that the properties of RA are often somewhat degraded compared with natural aggregate. The improvement of the physical and mechanical strength of recycled concrete has become a hot issue in the research of recycled concrete. Accelerated carbonation can effectively improve the strength of concrete, and steam curing can improve the impermeability of recycled concrete [8, 9]. Deng et al. applied recycled coarse aggregate to cement stabilized base and studied the influence of RA homogeneity on cement stabilized base [10]. Many scholars have also carried out corresponding studies on the application and reinforcement of RA. Among them, fly ash as industrial waste is also a concern by many scholars. Some scholars have found that fly ash pore refinement is beneficial to offset the higher porosity of RA by means of microscopic tests. In addition, fly ash has a positive effect on the erosion resistance of recycled concrete [11, 12]. The research of most scholars has shown that the appropriate addition of fly ash is helpful for the application of RA in engineering. To sum up, although there are many related researches on the application of RA in China, these researches are mainly focused on non-load-bearing concrete and semirigid base materials. The characteristics of different road engineering materials are quite different. Although the existing research results have certain reference significance, it is difficult to directly apply to roadbed reinforcement projects.

Several production technologies capable of manufacturing high-quality RA have been developed, and the recycled coarse aggregate concrete were applied to the upper structure of buildings on a trial basis particularly in Japan [13, 14]. In some Southern European countries, most RA are used in road construction and unpaved rural roads [15]. These uses have little added value but are a good alternative for RA with medium or low quality [16]. High-quality RA with high recycling potential can be obtained using selective dismantling techniques [17]. The use of these high-quality aggregates in the manufacture of concrete and mortar gives more added value to these recycled materials. In addition, the TOPSIS analysis method can comprehensively analyze the optimal solution of each parameter under multifactor conditions [18].

Table 1: Physical properties of RCA and RMA.

Aggregate type	Apparent density (kg/m^3)	Micro powder content (%)	Needle-like content (%)	Crush value (%)	Water absorption (%)
RCA	2.59	1.5	5.3	27.3	5.8
RMA	2.39	2.1	6.1	40.8	11.2

In this paper, recycled concrete aggregate (RCA) and recycled macadam aggregate (RMA) are the research objects. The compressive strength, hydration characteristics, and frost resistance were used as evaluation indexes to analyze the influence of RA content on the material properties of dry-mixed cement RA pile. At the same time, based on the characteristics of low hydration heat and durability improvement of fly ash, this paper systematically studied the influence of different fly ash content on compressive strength, hydration characteristics, and frost resistance of dry-mixed cement RA pile. Based on the requirements of roadbed reinforcement on the material strength, hydration heat release, and freezing resistance of dry-mixed cement RA piles, TOPSIS analysis method was used to comprehensively evaluate dry-mixed cement recycled piles prepared from different types of RA, and to explore the regeneration of dry-mixed cement. The optimal composition of aggregate piles provides corresponding reference for its engineering application.

2. Materials and Test Methods

2.1. Raw Materials. The raw materials used for preparing the CCG and CMG included ordinary Portland cement, mineral admixture, fine aggregates, RCA, and RMA. The morphology of RCA and RMA is shown in Figure 1, and the physical performance indicators of RCA and RMA are shown in Table 1. The physical properties of Portland cement are shown in Table 2. The chemical composition of industrial-grade fly ash (FA) is shown in Table 3. The fineness modulus of fine aggregate is 3.3, and its performance indicators are shown in Table 4.

In order to study the effect of RA content on the performance of CCG and CMG, the content of RCA and RMA

Table 2: Physical properties of cement.

Cement fineness (%)	Setting time		Compressive strength (MPa)		Flexural strength (MPa)		Stability (mm)
	Initial setting (min)	Final setting (h)	3 d	28 d	3 d	28 d	
2.3	165	5.5	12.6	35.0	2.9	6.1	1.5

Table 3: Chemical composition of considered FA (wt. %).

Al_2O_3	SiO_2	MgO	K_2O	CaO	Fe_2O_3	P_2O_5	SO_3	Na_2O
22.0	52.68	0.6	1.98	8.53	11.8	0.94	1.12	0.35

Table 4: Physical properties of fine aggregate.

Fineness modulus	Bulk density (kg/m^3)	Apparent density (kg/m^3)	Void ratio (%)	Stone powder content (%)	Crush indicator (%)
3.3	1447	2700	40	4.1	13

was 0, 20%, 40%, 60%, 80%, and 100%, numbered NC, RCA-20, RCA-40, RCA-60, RCA-80, RCA-100, RMA-20, RMA-40, RMA-60, RMA-80, and RMA-100, respectively. The mixing proportion of CCG and CMG is shown in Table 5. In order to study the effect of FA content on the performance of CCG and CMG, the content of FA was 0, 10%, 20%, and 30%, numbered RCA20F10, RCA20F20, RCA20F30, RMA20F10, RMA20F20, and RMA20F30, respectively. The mixing proportion of CCG and CMG is shown in Table 6.

2.2. Specimen Preparation. The test process includes the following steps: (1) the suitable amount coarse and fine aggregates are placed in a rectangular pan with a size of 400 mm × 600 mm × 70 mm; (2) the dry materials are mixed evenly for 3 min; (3) the water is poured into the dry ingredients and whisk quickly for 5 min; (4) add the suitable amount cement to the stuffed mixture and mix well for 6 min; (5) put the wet material into a square test mould with a side length of 100 mm; (6) according to the specification "*Testing Methods of Cement and Concrete for Highway Engineering*" [19], cure for 1 d and then demould.

2.3. Test Methods

2.3.1. Compressive Strength. According to the specification "*Standard for Test Method of Concrete Physical and Mechanical Properties*" [20], the compressive strength test was carried out on the samples of standard curing 7 d, 28 d, and 90 d respectively, and each sample was tested 3 times, and the average value was calculated as the final result.

2.3.2. Heat of Hydration. The heat of hydration of CCG and CMG was obtained by curing a specimen with a moulding size of 100 mm × 100 mm × 100 mm using box curing for 24 d, under the temperature of 20°C ± 2°C and a relative humidity of 90% ± 5%, according to the standard "*Test Methods for Heat of Hydration of Cement*" [21]. The PTS-12S hydration heat tester was used in the experiment.

2.3.3. Mass Loss Rate. Cubes with a side length of 150 mm were subjected to freeze-thaw cycles according to the specification "*Standard for Test Methods of Long-term Performance and Durability of Ordinary Concrete*" [22]. The mass of exfoliation (m_s) and the mass loss rate (γ) of the specimen are computed using the formula below for the specimen after freeze-thaw cycles.

$$m_s = m_b - m_f \tag{1}$$

$$\gamma = \frac{m_s}{m} \tag{2}$$

where m_s is mass of exfoliation of specimen. m_b is the total mass of filter paper and peel after drying; m_f is the filter paper quality; m is the mass of the dried specimen.

2.3.4. Relative Dynamic Elastic Modulus. The relative dynamic elastic modulus of the samples was tested according to specification "Test Methods of Cement and Concrete for Highway Engineering" [19]. The test was carried out with a cuboid specimen of 100 mm × 100 mm × 400 mm, and the frequency was set to 100 Hz.

3. Results and Discussion

3.1. Effects of RA Substitution Rate on Material Properties

3.1.1. Compressive Strength. The test results of different substitution rates on the compressive strength of CCG and CMG are shown in Figure 2. It can be seen from Figure 2 that, with the increase of the replacement rate, the strength of the dry-mixed cement aggregate pile decreases gradually. This may be related to the old mortar in the outer layer of RA [13, 14]. There are a lot of micro-cracks in the old mortar, and the internal structure is more easily damaged when it is subjected to external pressure. It can be seen from Table 4 that the crushing value of RCA is 27.3%; the crushing value of MCA is 40.8%. The aggregate acts as a scaffold in the dry-mixed cement aggregate pile, and the destruction of the aggregate reduces the overall compressive strength [15]. Therefore, the compressive strength of the dry-mixed

Table 5: The mixing proportion of CCG and CMG.

No.	Cement (kg/m^3)	Effective water (kg/m^3)	Additional water (kg/m^3)	W/C	Stone chips (kg/m^3)	Gravel kg/m^3
NC	480	240.0	0	0.5	1297	1584
RCA-20		259.2	6.65	0.54		
RCA-40		273.3	13.31	0.57		
RCA-60		292.8	19.96	0.61		
RCA-80		312.0	26.61	0.65		
RCA-100		331.2	33.26	0.69		
RMA-20		259.2	6.65	0.54		
RMA-40		273.3	13.31	0.57		
RMA-60		292.8	19.96	0.61		
RMA-80		312.0	26.61	0.65		
RMA-100		331.2	33.26	0.69		

Table 6: The mixing proportion of CCG and CMG.

No.	FA content (%)	Cement (kg/m^3)	Sand (kg/m^3)	Gravel (kg/m^3)	Additional water (kg/m^3)	Free water (kg/m^3)
RCA20F10	26	228	595	1103	113	194
RCA20F20	52	202				
RCA20F30	77	177				
RMA20F10	26	228				
RMA20F20	52	202				
RMA20F30	77	177				

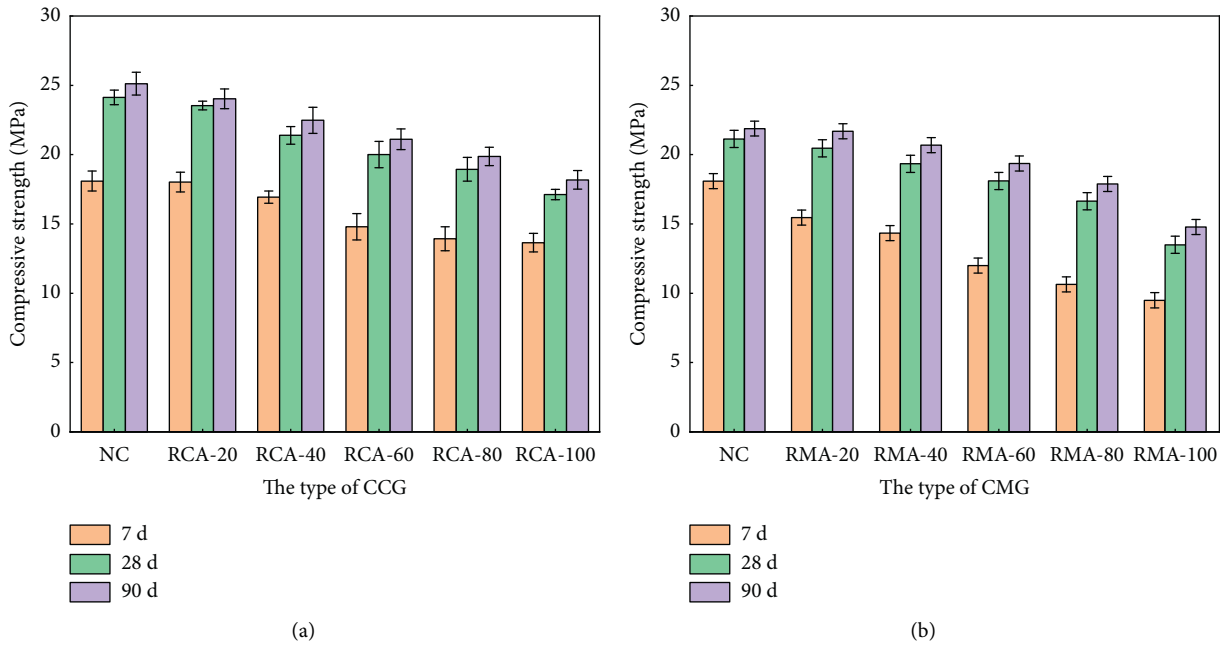

Figure 2: The effect of RCA and RMA with different dosages on compressive strength of CCG and CMG. (a) CCG, (b) CMG.

cement recycled aggregate pile gradually decreases with the increase of the amount of recycled aggregate. In contrast, the compressive strength of CMG is lower than that of CCG due to the lower crush value of RMA and the higher water absorption of RMA, which is about two times that of RCA.

3.1.2. Heat of Hydration. The experimental results of the heat of hydration of CCG and CMG with different substitution rates are shown in Figure 3. According to Figure 3, with the increase of the replacement rate of RA, the heat of hydration of CCG and CMG also increases. It can be found from Table 5 that, due to the high water absorption of RA, a part of additional water is required for prewetting treatment [16]. Besides, with the increase of the replacement rate of RA, the required water consumption is also increasing, resulting in an increasing water-cement ratio. The cement paste with low water-cement ratio has smaller porosity and smaller pore size, so the cement paste is denser. In order for cement to be

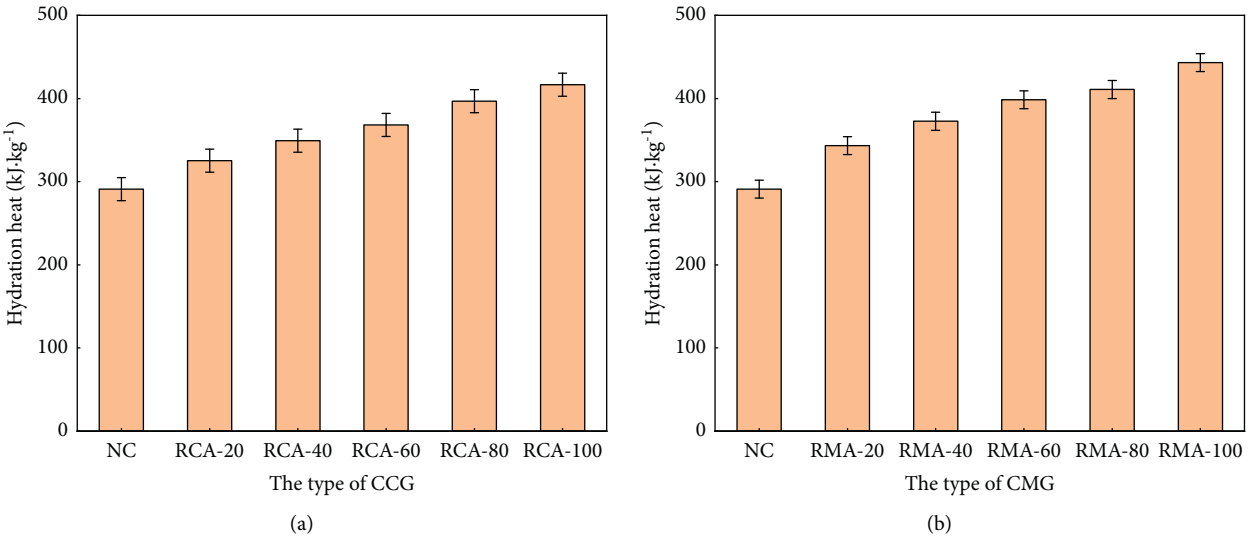

Figure 3: The effect of RCA and RMA with different dosages on hydration heat of CCG and CMG. (a) CCG, (b) CMG.

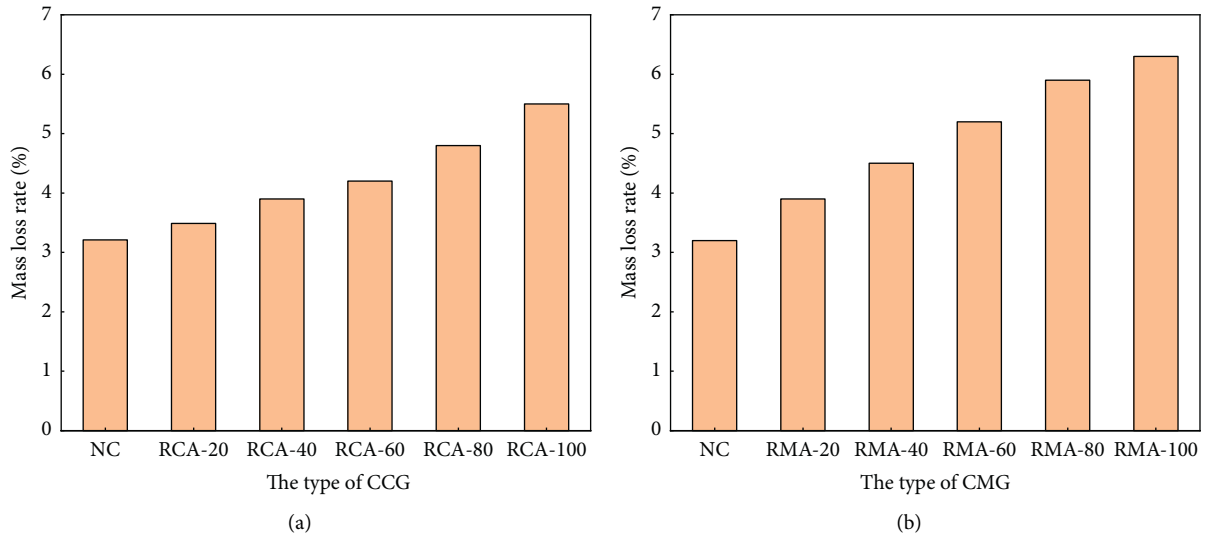

Figure 4: The effect of RCA and RMA with different dosages on mass loss rate of CCG and CMG. (a) CCG, (b) CMG.

fully hydrated, sufficient water diffusion in the slurry is required [17]. Therefore, the heat of hydration of the sample with a smaller water-cement ratio is also smaller; in other words, the heat of hydration of the sample with a higher replacement rate of recycled aggregate is also larger. Compared to CCG, CMG has a higher heat of hydration. The hydration exotherm is not only affected by the degree of hydration, but also closely related to the initial water content [18]. It can be seen from Table 4 that the water absorption rate of RCA is 5.8%, and that of RMA is 11.2%. Due to the high water absorption, the additional water gives the CMG a higher initial water content, resulting in a higher heat of hydration for the CMG. In conclusion, CCG shows better performance in terms of heat of hydration.

3.1.3. Frost Resistance. The test results of different RA substitution rates on the mass loss rate of CCG and CMG are shown in Figure 4. Figure 4 shows that when the replacement rate of recycled aggregate increases, the mass loss rate increases as well. This is owing to recycled aggregates' high crushing value and low apparent density, which makes them more prone to damage [23, 24]. On the one hand, the high water absorption rate of RA causes it to absorb part of the water, and frost heave occurs during the freezing and thawing process, resulting in structural damage and loss. On the other hand, the bonding strength of RA is weaker than that of natural aggregate, and it is not easy to bond with old and new mortar, so the frost resistance is worse [25].

The experimental results of the relative dynamic elastic modulus of RCA and RMA with different RA substitution rates are shown in Figure 5. The relative dynamic elastic modulus

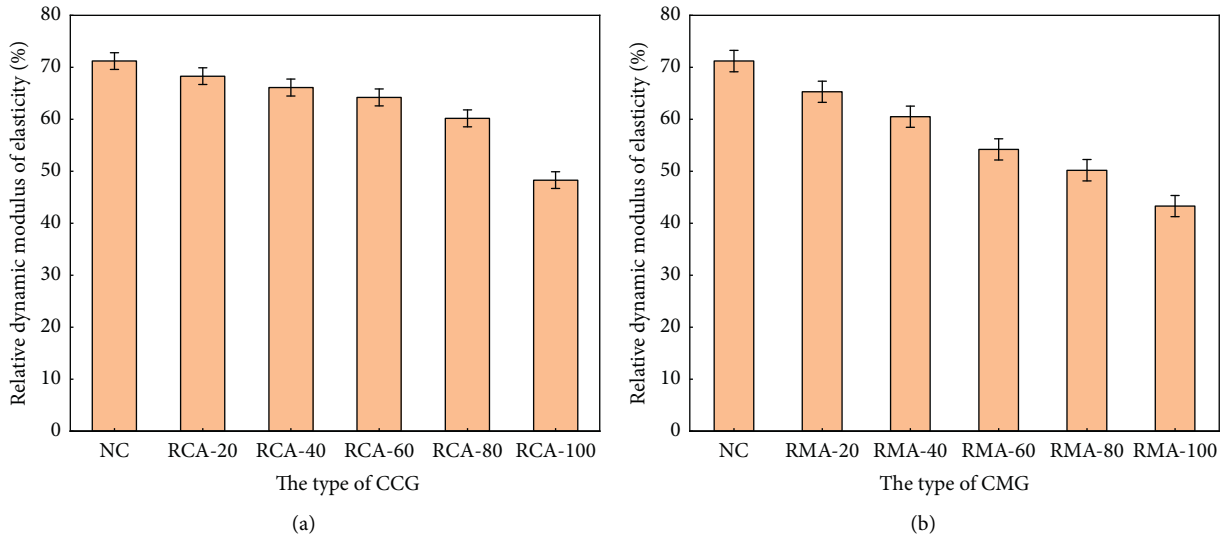

Figure 5: The effect of RCA and RMA with different dosages on relative dynamic elastic modulus of CCG and CMG. (a) CCG, (b) CMG.

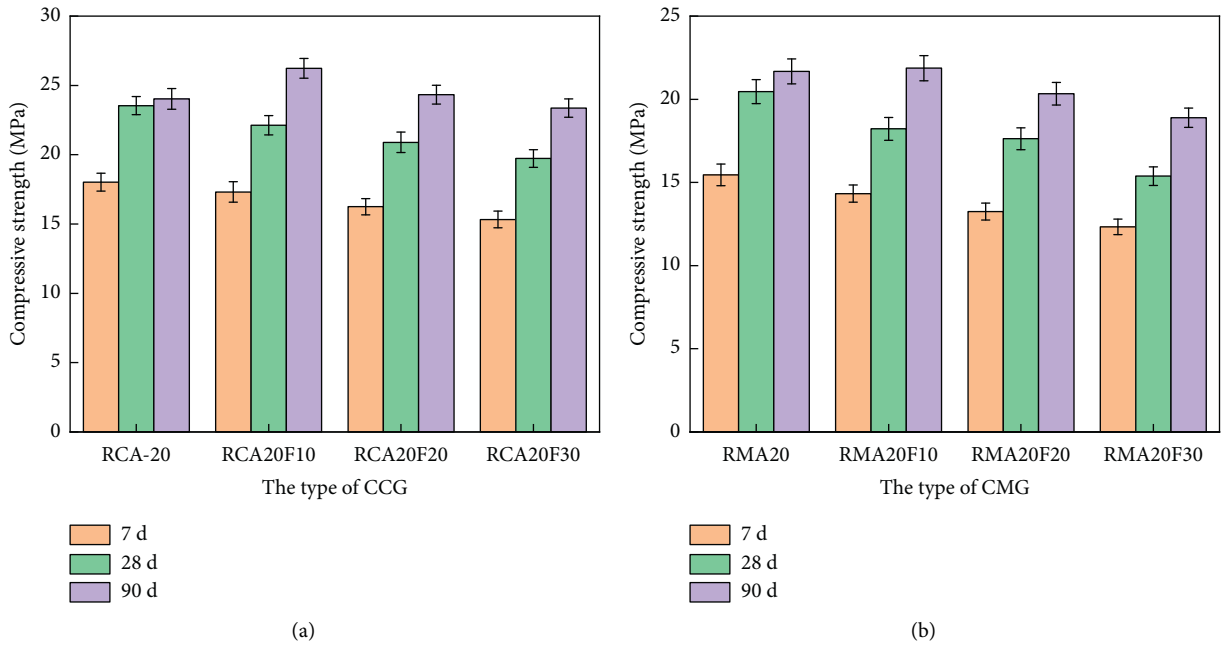

Figure 6: The compressive strength of CCG and CMG with different content of fly ash. (a) CCG, (b) CMG.

rapidly falls as the RA content increases, as seen in Figure 5. The high crushing value and low apparent density of RA, like the mass loss rate, render the interior structure of CCG and CMG prone to destruction. RMA has a rougher surface and more pores than RCA, as seen in Figure 1. Table 4 shows that RCA has a higher apparent density than RMA, as well as a lower crush value and water absorption. In conclusion, CCG has a higher relative dynamic elastic modulus than CMG.

3.2. Effect of fly Ash Content on the Performance of Dry Mix Cement RA Pile

3.2.1. Compressive Strength. The compressive strength of CCG and CMG with different content of fly ash is shown in Figure 6. From Figure 6, the compressive strength of CCG and CMG decreases at 7 d and 28 d due to the slow hydration of fly ash in the early stages, which cannot provide enough strength for CCG and CMG [26]. However, the AFt crystals and CH crystals are generated after the secondary hydration reaction of fly ash, contributing to an increase in compressive strength at 90 d [27]. Furthermore, with the increase of fly ash, the compressive strength of CCG and CMG at 90 d shows a trend of first increasing and then declining. The high fly ash content can cause problems such as low strength and carbonation of concrete at an early stage [28]. Meanwhile, excessive amounts of fly ash can decrease the workability and compressive strength of concrete (Temesge et al.) [29]. The reason for this phenomenon is the excessive water requirement of fly ash in large content, and the secondary

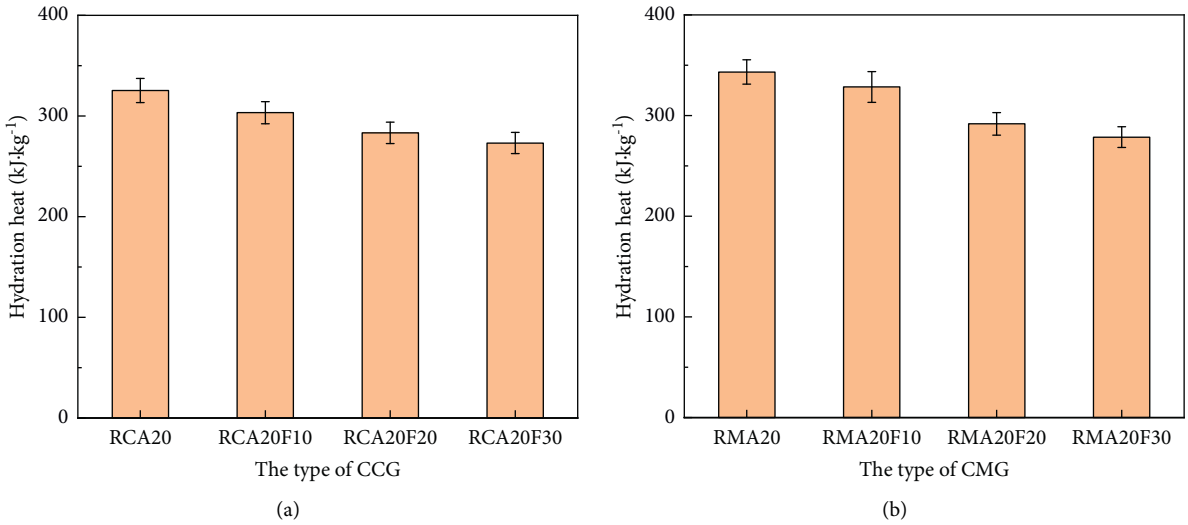

Figure 7: The hydration heat of CCG and CMG with different content of fly ash. (a) CCG, (b) CMG.

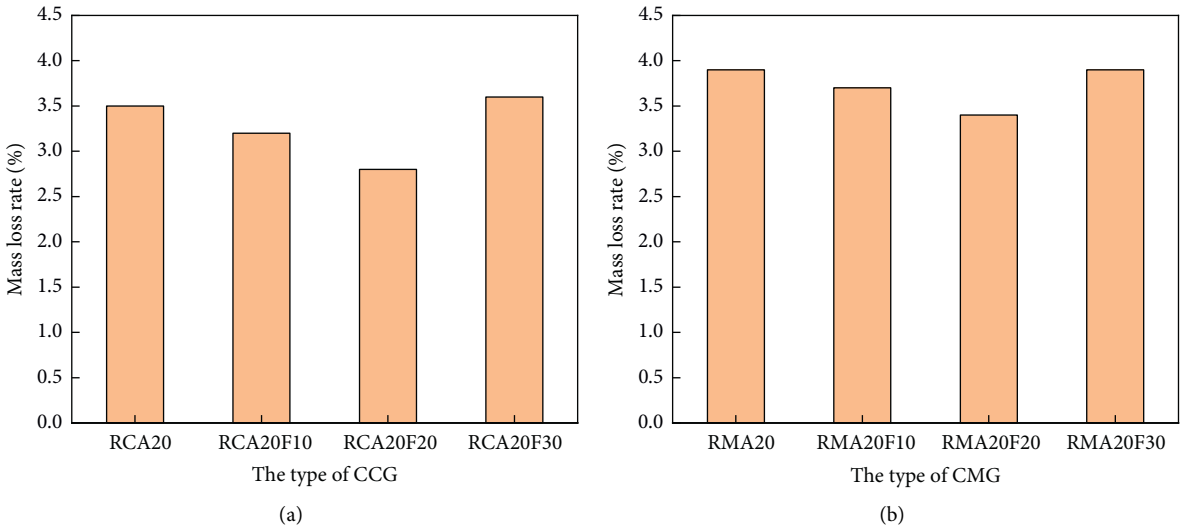

Figure 8: The mass loss rate of CCG and CMG with different content of fly ash. (a) CCG, (b) CMG.

hydration is incomplete. It can be found that the compressive strength is higher when the CCG replacement rate is 20%, and the fly ash content is 10%.

3.2.2. Hydration Heat. The results of fly ash content on the hydration heat of CCG and CMG are shown in Figure 7. The hydration heat of CCG and CMG will gradually decrease with the increase of fly ash [30]. The generation of hydration heat mainly comes from the heat release from the cement hydration reaction. The cement content of the hydration reaction in the early stage and the hydration heat is reduced by using fly ash instead of cement, and this result is consistent with the conclusion of other studies [27, 31].

3.2.3. Frost Resistance. Figures 8 and 9 show the test results of fly ash content on the frost resistance of CCG and CMG. According to Figures 8 and 9, the mass loss rate decreases and then increases with the increase of fly ash content, and the relative dynamic elastic modulus exhibited a trend of rising and then falling. Moreover, using fly ash as the filler will help fill gaps in the dry-mixed cement recycled aggregate pile, improving structural compactness and providing frost resistance [32, 33]. As a result, too much fly ash will reduce the strength of CCG and CMG in the early stage, resulting in higher water demands and a more vulnerable internal structure to freeze-thaw damage. The internal structure is not tight enough, and the frost resistance is reduced. RCA with 20% fly ash content has a lower mass loss rate and a higher relative dynamic elastic modulus.

3.3. The Comprehensive Performance Evaluation of Dry-Mixed RA Piles

3.3.1. The Analysis of TOPSIS. TOPSIS analysis method first normalizes the original data matrix and then determines the

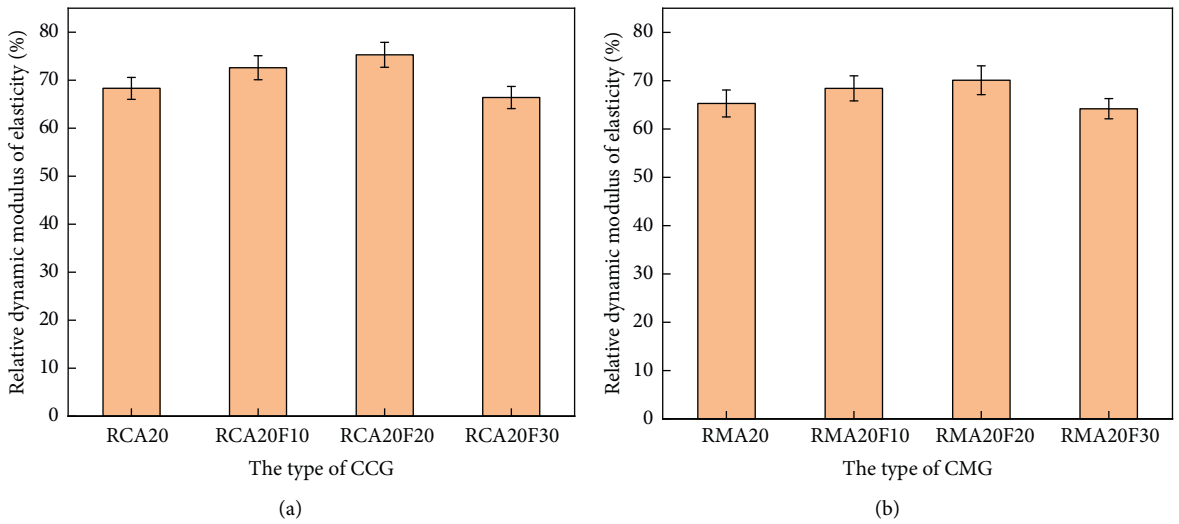

Figure 9: The relative dynamic modulus of elasticity of CCG and CMG with different content of fly ash. (a) CCG, (b) CMG.

optimal and inferior solutions among a finite number of solutions through the optimal vector and inferior vector. Then, it determines the closeness of each study factor of the object of investigation relative to the optimal solution by comparing the object of investigation with the optimal and inferior solutions and then evaluates the superiority and inferiority of the object of investigation [34, 35]. The specific steps are as follows.

In the first step, a decision matrix needs to be constructed, and the raw data can be represented by matrix $X = (X_{ij})_{n\times m}$, where n and m represent the number of evaluation objects and evaluation indicators, respectively. The resulting raw data are matrixed by

$$Z_{ij} = \frac{X_{ij}}{\sqrt{\sum_{i=1}^{m} X_{ij}^2}} \tag{3}$$

In the second step, the above obtained matrix is normalized by Eq. (4) and Eq. (5); then, determine the optimal vector and the worst vector.

$$Y^+ = \left(Y_{\max 1}, Y_{\max 2}, \cdots, Y_{\max m}\right) \tag{4}$$

$$Y^- = \left(Y_{\min 1}, Y_{\min 2}, \cdots, Y_{\min m}\right) \tag{5}$$

In the third step, the difference distance between the i^{th} examined object and the optimal solution and the worst solution is then determined by Eq. (6) and Eq. (7).

$$D_i^+ = \sqrt{\sum_{j=1}^{m} \left(X_{\max j} - Y_{ij}\right)^2} \tag{6}$$

$$D_i^- = \sqrt{\sum_{j=1}^{m} \left(X_{\min j} - Y_{ij}\right)^2} \tag{7}$$

In the fourth step, the similarity between each examined object and the optimal solution is calculated by Eq. (8) and ranked for comparison to determine the optimal solution.

$$CI = D_i^- / \left(D_i^+ + D_i^-\right) 1 \le i \le n \tag{8}$$

3.3.2. Analysis of Calculation Results. Compressive strength, hydration heat, and frost resistance are used as the investigating factors to achieve a comprehensive evaluation of CCG and CMG. The results of experimental values of compressive strength, the heat of hydration, mass loss, and relative dynamic modulus of elasticity are shown in Table 7.

(1) The above experimental data are matrixed by Eq. (3), and the resulting standard matrix is as follows:

$$\begin{pmatrix}
0.2850 & 0.3466 & 0.3241 & 0.2715 \\
0.2726 & 0.2687 & 0.2927 & 0.2605 \\
0.2550 & 0.2140 & 0.2614 & 0.2521 \\
0.2390 & 0.1707 & 0.2300 & 0.2448 \\
0.2254 & 0.1060 & 0.1568 & 0.2296 \\
0.2062 & 0.0604 & 0.0523 & 0.1842 \\
0.2460 & 0.2277 & 0.2509 & 0.2490 \\
0.2347 & 0.1609 & 0.1882 & 0.2307 \\
0.2196 & 0.1019 & 0.1150 & 0.2067 \\
0.2028 & 0.0738 & 0.0418 & 0.1914 \\
0.1677 & 0 & 0 & 0.1651 \\
0.2976 & 0.3188 & 0.3241 & 0.2605 \\
0.2760 & 0.3646 & 0.3659 & 0.2769 \\
0.2650 & 0.3877 & 0.2823 & 0.2872 \\
0.2481 & 0.2277 & 0.2718 & 0.2609 \\
0.2306 & 0.2616 & 0.3032 & 0.2673 \\
0.2143 & 0.3450 & 0.2509 & 0.2448
\end{pmatrix} \tag{9}$$

(2) The optimal vector and the worst vector obtained by Eq. (4) and Eq. (5) are as follows:

Table 7: Factor values for CCG and CMG.

Number	90 d compressive strength (MPa)	The heat of hydration (kJ/kg)	Mass loss (%)	Relative dynamic modulus of elasticity (%)
NC	25.12	291.1	3.2	71.2
RCA20	24.03	325.3	3.5	68.3
RCA40	22.48	349.3	3.8	66.1
RCA60	21.11	368.3	4.1	64.2
RCA80	19.87	396.7	4.8	60.2
RCA100	18.18	416.7	5.8	48.3
RMA20	21.68	343.3	3.9	65.3
RMA40	20.69	372.6	4.5	60.5
RMA60	19.36	398.5	5.2	54.2
RMA80	17.88	410.8	5.9	50.2
RMA100	14.78	443.2	6.3	43.3
RCA20F10	26.23	303.3	3.2	68.3
RCA20F20	24.33	283.2	2.8	72.6
RCA20F30	23.36	273.1	3.6	75.3
RMA20F10	21.87	343.3	3.7	68.4
RMA20F20	20.33	328.4	3.4	70.1
RMA20F30	18.89	291.8	3.9	64.2

Table 8: Sorting index values for different types of recycled aggregate materials.

Aggregate type	D^+	D^-	Similarity CI
NC	0.0619	0.5003	0.8899
RCA20	0.1444	0.4219	0.7450
RCA40	0.2101	0.3596	0.6312
RCA60	0.2659	0.3059	0.5349
RCA80	0.3628	0.2081	0.3646
RCA100	0.4737	0.0907	0.1607
RMA20	0.2072	0.3577	0.6332
RMA40	0.3002	0.2648	0.4686
RMA60	0.3965	0.1674	0.2969
RMA80	0.4708	0.0956	0.1687
RMA100	0.5621	0	0
RCA20F10	0.0848	0.4823	0.8504
RCA20F20	0.0332	0.5395	0.9421
RCA20F30	0.0898	0.5043	0.8489
RMA20F10	0.1939	0.3760	0.6598
RMA20F20	0.1571	0.4181	0.7268
RMA20F30	0.1542	0.4365	0.7390

$$Y^+ = (0.2976, 0.3877, 0.3659, 0.2872) \quad (10)$$

$$Y^- = (0.1677, 0, 0, 0.1651) \quad (11)$$

The difference distance and similarity between each examined object and the optimal solution are obtained by Eq. (7) and Eq. (8). The obtained results are shown in Table 8.

Table 8 shows that, through the TOPSIS analysis method, the piles with 20% fly ash added scored the highest, even exceeding the score of natural aggregates after a comprehensive analysis of compressive strength, exothermic hydration, and frost resistance indexes. In comparing the properties of recycled materials, it is concluded that RCA > RMA considering the compressive strength, exothermic hydration, and frost resistance.

4. Conclusion

(1) The mechanical properties and freezing resistance of CCG and CMG gradually deteriorate with RCA and RMA substitution rates. Meanwhile, the exothermic hydration of CCG and CMG increases continuously with the increase of the substitution rate.

(2) RCA has a higher crushing value and lower water absorption than RMA. CCG prepared by RCA has higher compressive strength, frost resistance and lower hydration heat than CMG prepared by CMG.

(3) The use of fly ash to replace part of cement improves the late compressive strength and frost resistance of CCG and CMG and lowers the hydration heat and material cost.

(4) TOPSIS analysis of dry-mix cement recycled aggregate piles based on mechanical properties, frost resistance, and exothermic hydration capacity demonstrated that the comprehensive score initially increases and then decreases with fly ash. When the CCG substitution rate reaches 20%, the composite score of CCG mixed with 20% fly ash is higher than that of the conventional dry-mix cement aggregate pile material, which has better performance.

Data Availability

The data used to support the findings of this study are included within the article.

Conflicts of Interest

The authors declare no conflicts of interest.

Acknowledgments

This research was supported by Science and Technology Project of Housing and Urban Rural Development Department of Shaanxi Province (2020-K11), Shaanxi Huashan Road and Bridge Group Co., Ltd. Technology Project (No. HSLQ-KYHT-2020-002), and Shaanxi Province Key R&D Program (No. 2021SF-514).

References

[1] E. M. B. De Guzman and M. C. Alfaro, "Laboratory-scale model studies on corduroy-reinforced road embankments on peat foundations using transparent soil," *Transportation Geotechnics*, vol. 16, pp. 1–10, 2018.

[2] J. Liu, T. Zhang, H. Guo, Z. Wang, and X. Wang, "Evaluation of self-healing properties of asphalt mixture containing steel slag under microwave heating: mechanical, thermal transfer and voids microstructural characteristics," *Journal of Cleaner Production*, vol. 342, p. 130932, 2022.

[3] J. Zhang, "Numerical Simulation of soft roadbed reinforced by dry cement gravel pile," *Highway*, vol. 66, no. 04, pp. 18–22, 2021, (in Chinese).

[4] S. Li, Y. Fang, and X. Wu, "A systematic review of lean construction in Mainland China," *Journal of Cleaner Production*, vol. 257, p. 120581, 2020.

[5] G. Bai, C. Zhu, C. Liu, and B. Liu, "An evaluation of the recycled aggregate characteristics and the recycled aggregate concrete mechanical properties," *Construction and Building Materials*, vol. 240, no. 240, p. 117978, 2020.

[6] M. S. Bidabadi, M. Akbari, and O. Panahi, "Optimum mix design of recycled concrete based on the fresh and hardened properties of concrete," *Journal of Building Engineering*, vol. 32, p. 101483, 2020.

[7] Q. Liu, J. Xiao, Z. Pan, and L. Li, "Modeling of recycled concrete with waste Concrete aggregate and waste brick Aggregate," *Journal of Building Structures*, vol. 41, no. 12, pp. 133–140, 2020, (in Chinese).

[8] J. Park, J. Lee, C.-W. Chung, S. Wang, and M. Lee, "Accelerated carbonation of recycled aggregates using the pressurized supercritical carbon dioxide sparging process," *Minerals*, vol. 10, no. 6, p. 486, 2020.

[9] S. Zhuang and J. Sun, "The feasibility of properly raising temperature for preparing high-volume fly ash or slag steam-cured concrete: an evaluation on DEF, 4-year strength and durability," *Construction and Building Materials*, vol. 242, p. 118094, 2020.

[10] C. Deng, Y. Chen, H. Chen, B. Guan, and Z. Sun, "Research on homogeneity evaluation and control technology of reclaimed coarse aggregate for cement stabilized base," *Highway*, vol. 65, no. 09, pp. 251–255, 2020, (in Chinese).

[11] B. Ali, S. S. Raza, R. Kurda, and R. Alyousef, "Synergistic effects of fly ash and hooked steel fibers on strength and durability properties of high strength recycled aggregate concrete," *Resources, Conservation and Recycling*, vol. 168, p. 105444, 2021.

[12] S. Sunayana and S. V. Barai, "Partially fly ash incorporated recycled coarse aggregate based concrete: microstructure perspectives and critical analysis," *Construction and Building Materials*, vol. 278, p. 122322, 2021.

[13] A. Shintani, K. Yoda, T. Onodera, and Y. Kawanishi, "On-site application of two types of recycled course aggregate concrete," *Annual report of JCI*, vol. 28, no. 1, pp. 1463–1468, 2006, (in Japanese).

[14] E. Kawai, K. Yanagibashi, T. Iwashimizu, and H. Takiguchi, "Application of recycled aggregate concrete to building project: example of Shin-Senri Sakuragaoka renovation project," *Concrete J*, vol. 44, no. 2, pp. 46–53, 2006, (in Japanese).

[15] F. Agrela, A. Barbudo, A. Ramírez, J. Ayuso, M. D. Carvajal, and J. R. Jiménez, "Construction of road sections using mixed recycled aggregates treated with cement in Malaga, Spain," *Resources, Conservation and Recycling*, vol. 58, pp. 98–106, 2012.

[16] J. R. Jiménez, J. Ayuso, F. Agrela, M. López, and A. P. Galvín, "Utilisation of unbound recycled aggregates from selected CDW in unpaved rural roads," *Resources, Conservation and Recycling*, vol. 58, pp. 88–97, 2012.

[17] J. Jiménez, J. Ayuso, A. Galvín, M. López, and F. Agrela, "Use of mixed recycled aggregates with a low embodied energy from non-selected CDW in unpaved rural roads," *Construction and Building Materials*, vol. 34, pp. 34–43, 2012.

[18] H. Shen, L. Hu, and K. K. Lai, "A mathematical programming model to determine objective weights for the interval extension of TOPSIS," *Mathematical Problems in Engineering*, vol. 2018, pp. 1–6, 2018.

[19] Ministry of Transport 2020, *Testing Methods of Cement and Concrete for Highway Engineering*, Ministry of Transport of the People's Republic of China, 2020.

[20] Gb/T 50081-2019, *Standard for Test Method of concrete Physical and Mechanical Properties*, Ministry of Housing and Urban-Rural Development of the People's Republic of China, 2019.

[21] Gb/T 18046-2008, *Test Methods for Heat of Hydration of Cement*, General Administration of Quality Supervision and Quarantine of the People's Republic of China, 2008.

[22] Gb/T 50082-2009, *Standard for Test Methdos of Long-Term Performance and Durability of Ordinary Concrete*, Ministry of Housing and Urban-Rural Development of the People's Republic of China, 2009.

[23] H. Dabiri, M. Kioumarsi, A. Kheyroddin, A. Kandiri, and F. Sartipi, "Compressive strength of concrete with recycled aggregate; a machine learning-based evaluation," *Cleaner Materials*, vol. 3, p. 100044, 2022.

[24] Q. Zhu, Y. X. Yuan, J. H. Chen, L. Fan, and H. Yang, "Research on the high-temperature resistance of recycled aggregate concrete with iron tailing sand," *Construction and Building Materials*, vol. 327, p. 126889, 2022.

[25] A. İ. Uğurlu, M. B. Karakoç, and A. Özcan, "Effect of binder content and recycled concrete aggregate on freeze-thaw and sulfate resistance of GGBFS based geopolymer concretes," *Construction and Building Materials*, vol. 301, p. 124246, 2021.

[26] H. Li, Z. Ban, H. Qin, L. Ma, and G KingWang, "A heteromeric membrane-bound prenyltransferase complex from hop catalyzes three sequential aromatic prenylations in the bitter acid pathway," *Plant physiology*, vol. 167, no. 3, pp. 650–659, 2015, (in Chinese).

[27] M. Farzad, S. Vute, and V. Kirk, "The effect of fly ash fineness on heat of hydration, microstructure, flow and compressive strength of blended cement pastes," *Case Studies in Construction Materials*, vol. 10, pp. 152–159, 2019.

[28] D. Florian, W. Frank, L. Barbara et al., "Hydration of Portland cement with high replacement by siliceous fly ash[J]," *Cement and Concrete Research*, vol. 42, no. 10, pp. 1389–1400, 2012.

[29] T. Fantu, G. Alemayehu, G. Kebede, Y. Abebe, S. K. Selvaraj, and V. Paramasivam, "Experimental investigation of compressive strength for fly ash on high strength concrete C-55 grade," *Materials Today Proceedings*, vol. 46, pp. 7507–7517, 2021.

[30] W. Chen, Y. Zhou, S. Li, and P. Yan, "Impact of temperature rising inhibitor on hydration of cement-fly ash cementitious materials and performance of concrete," *Journal of the Chinese Ceramic Society*, vol. 49, no. 08, pp. 1609–1618, 2021.

[31] Z. Giergiczny, "Fly ash and slag," *Cement and Concrete Research*, vol. 124, p. 105826, 2019.

[32] L. Xiao and J. Li, "Study on the effect of straw fiber, fly ash and diatomite on mechanical property and frost resistance of straw cement-based material," *New Chemical Materials*, vol. 49, no. 06, pp. 236–239, 2021, (in Chinese).

[33] J. Liu, L. Qi, X. Wang, M. Li, and Z. Wang, "Influence of aging induced by mutation in temperature on property and microstructure development of asphalt binders," *Construction and Building Materials*, vol. 319, p. 126083, 2022.

[34] I. Basheleishvili, "Developing the expert decision-making algorithm using the methods of multi-criteria analysis," *Cybernetics and Information Technologies*, vol. 20, no. 2, pp. 22–29, 2020.

[35] S. Hasnain, M. K. Ali, J. Akhter, B. Ahmed, and N. Abbas, "Selection of an industrial boiler for a soda-ash production plant using analytical hierarchy process and TOPSIS approaches," *Case Studies in Thermal Engineering*, vol. 19, p. 100636, 2020.